Guided wave propagation in metallic and resin plates loaded with water on single surface

Cite as: AIP Conference Proceedings **1706**, 030003 (2016); https://doi.org/10.1063/1.4940475
Published Online: 10 February 2016

Takahiro Hayashi and Daisuke Inoue

Guided Wave Propagation in Metallic and Resin Plates Loaded with Water on Single Surface

Takahiro Hayashi[1, a)] and Daisuke Inoue[1]

[1]*Kyoto University*
Kyotodaigaku-katsura C3 bld., Nishikyo-ku, Kyoto 615-8540, Japan

[a)]Corresponding author: hayashi@kuaero.kyoto-u.ac.jp

Abstract. Our previous papers reported dispersion curves for leaky Lamb waves in a water-loaded plate and wave structures for several typical modes including quasi-Scholte waves [1,2]. The calculations were carried out with a semi-analytical finite element (SAFE) method developed for leaky Lamb waves. This study presents SAFE calculations for transient guided waves including time-domain waveforms and animations of wave propagation in metallic and resin water-loaded plates. The results show that non-dispersive and non-attenuated waves propagating along the interface between the fluid and the plate are expected for effective non-destructive evaluation of such fluid-loaded plates as storage tanks and transportation pipes. We calculated transient waves in both steel and polyvinyl chloride (PVC) plates loaded with water on a single side and input dynamic loading from a point source on the other water-free surface as typical examples of metallic and resin plates. For a steel plate, there exists a non-dispersive and non-attenuated mode, called the quasi-Scholte wave, having an almost identical phase velocity to that of water. The quasi-Scholte wave has superior generation efficiency in the low frequency range due to its broad energy distribution across the plate, whereas it is localized near the plate–water interface at higher frequencies. This means that it has superior detectability of inner defects. For a PVC plate, plural non-attenuated modes exist. One of the non-attenuated modes similar to the A0 mode of the Lamb wave in the form of a group velocity dispersion curve is promising for the non-destructive evaluation of the PVC plate because it provides prominent characteristics of generation efficiency and low dispersion.

INTRODUCTION

Semi-analytical finite element (SAFE) calculations have been developed as an efficient calculation technique for guided waves propagating in elongated structures such as plates and pipes [3–9]. Most of the SAFE calculations were formulated for guided waves in an elastic waveguide with homogeneous geometry and material constants in the longitudinal direction under the traction-free boundary conditions. However, practical objects to be inspected such as pipes and tanks often come in contact with media like fluid and soil, causing ultrasonic energy to leak. Hence, attenuation caused by the leakage is an indispensable issue.

Recently, SAFE calculations considering leaky media have become feasible by introducing absorbing layers and perfectly matched layers surrounding the leaky media or by expressing the outer open domain with the boundary element method [7–11]. SAFE calculations for leaky Lamb waves were formulated based on the characteristic that waves leaking into fluids propagate as plane harmonic waves with the sound speed of the fluids [1]. Moreover, SAFE calculations of transient responses for external dynamic loading were developed in Ref. [2].

Considering the inspection of pipes and tanks filled with water using guided waves, this study describes Lamb waves propagating in a plate loaded with water on a single surface. Dispersion curves, attenuation curves, wave structures, and transient responses for dynamic loading are calculated for steel and polyvinyl chloride plates as typical examples of metallic and resin plates. We discuss the detectability of inner defects in the walls of pipes or tanks.

42nd Annual Review of Progress in Quantitative Nondestructive Evaluation
AIP Conf. Proc. 1706, 030003-1–030003-7; doi: 10.1063/1.4940475

TRANSIENT WAVE CALCULATION FOR LEAKY LAMB WAVES

We consider a plate with a water-loaded lower surface and a traction-free upper surface on which the harmonic point force is loaded in the y direction at $x = 0$, with waves propagating in the plate and water. SAFE calculations for this condition were formulated based on the characteristic that a plane harmonic wave with the wavenumber of ξ_f $(= \omega / c_f)$ is generated by the Lamb wave with the x-directional wavenumber of ξ_x, where ω is the angular frequency and c_f is the wave speed of the fluid. Letting a nodal displacement vector at the cross-sectional nodes in frequency and wavenumber domains be $\mathbf{U}(\omega, \xi_x)$ and the y component of the wavenumber in the fluid ξ_f be ξ_y, the following governing equation is obtained:

$$\left(\mathbf{K}_1 + i\xi_x \mathbf{K}_2 + \xi_x^2 \mathbf{K}_3 - \omega^2 \mathbf{M} - \frac{\omega^2}{\xi_y} \mathbf{Q} \right) \mathbf{U} = \mathbf{F}^{ext} , \tag{1}$$

where $\mathbf{K}_1$, $\mathbf{K}_2$, $\mathbf{K}_3$, $\mathbf{M}$, and $\mathbf{Q}$ are known matrices calculated from the geometry and material constants, and $\mathbf{F}^{ext}$ is a vector determined by the external force. The wavenumbers ξ_x and ξ_y are related by the following equation:

$$\xi_x^2 + \xi_y^2 = \xi_f^2 . \tag{2}$$

Letting the external force vector be zero ($\mathbf{F}^{ext} = 0$), Eq. (1) is regarded as the following nonlinear eigenvalue problem with respect to ξ_x or ξ_y :

$$\left(\mathbf{K}_1 + i\xi_x \mathbf{K}_2 + \xi_x^2 \mathbf{K}_3 - \omega^2 \mathbf{M} - \frac{\omega^2}{\xi_y} \mathbf{Q} \right) \mathbf{U} = 0 . \tag{3}$$

In Ref. [1], this nonlinear eigenvalue equation was linearized using the characteristics of leaky Lamb waves, and solving the linear eigenvalue equation yields wavenumbers and wave structures for the Lamb wave modes. Moreover, in Ref. [2], the nodal displacement vector in the space domain was expressed by the sum of eigenmodes as

$$\mathbf{u} = \sum_m C^F{}_m \boldsymbol{\varphi}_m \exp(i\xi_{xm} x) , \tag{4}$$

where $C^F{}_m$ is the amplitude coefficient calculated from external loading conditions, and ξ_{xm} and $\boldsymbol{\varphi}_m$ are wavenumbers and wave structure vectors, respectively, obtained from the solution of Eq. (3), where m stands for the mth mode. The nodal displacement vector calculated using Eq. (4) in the frequency domain can be converted with an inverse fast Fourier transform to that in the time domain.

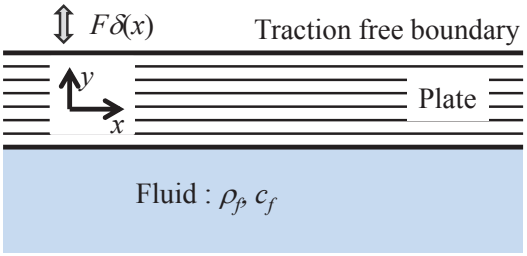

FIGURE 1. Geometrical conditions for SAFE calculations.

LAMB WAVES IN A METALLIC PLATE LOADED WITH FLUID ON A SINGLE SURFACE

First, a steel plate is investigated as a typical example of metallic plates. In this study, assuming transport pipes and storage tanks for water, a steel plate loaded with water on a single surface is considered. Figure 2 shows group velocity dispersion curves and attenuation curves for a steel plate with thickness d (longitudinal velocity c_L = 5900 m/s, transverse velocity c_T = 3200 m/s, density ρ_s = 7800 kg/m^3) coupled with water (sound velocity c_f = 1500 m/s,

density ρ_f = 1000 kg/m^3) on a single surface. The curves in Figs. 2(a) and 2(b) were derived from $c_g = \partial\omega/\partial\xi_x$ and $\mathrm{Im}(\xi_x)$, respectively, in which the complex wavenumber ξ_x is the solution of eigenvalue equation (3). Although an infinite number of Lamb wave modes exist in modal expansion theory with complex wavenumbers, these figures show the small attenuation modes of $\mathrm{Im}(\xi_x) < 200$. Physically unreasonable solutions for leaky Lamb waves, having infinitely large displacements at infinity of the water region, are also eliminated. Although the mode names S0 and A0 stand for symmetric and antisymmetric modes, respectively, for a plate with traction-free boundaries, these modes do not have perfectly symmetric and antisymmetric distributions with respect to the centerline of the plate due to the presence of water. The blue line represents the mode with zero attenuation, generally called the quasi-Scholte wave.

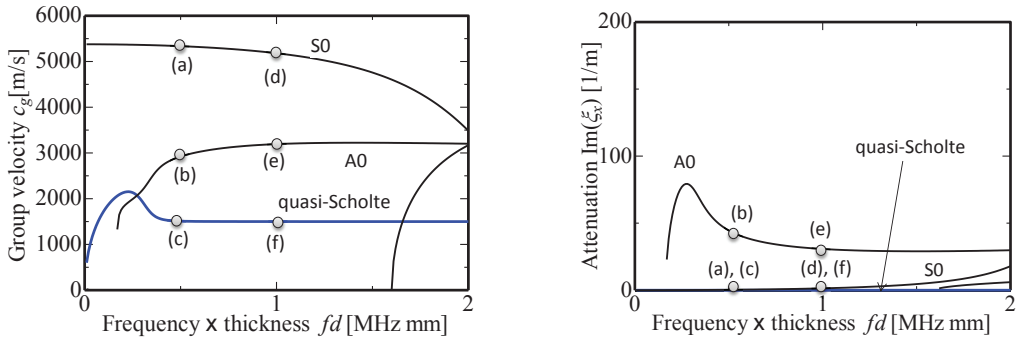

(a) Group velocity dispersion curves. (b) Attenuation curves.

FIGURE 2. Dispersion curves for a water-loaded steel plate.

Figure 3 shows the wave structures of the S0, A0, and quasi-Scholte modes at two different frequencies. These figures were calculated from the cross-sectional displacement vector φ_m that was used to derive an eigenvector of Eq. (3). The display ranges are 10d x 3d in the x and y directions, respectively, where the upper region of thickness d is a plate and the lower region of thickness 2d is water. The grid shift represents the displacements in the x and y directions and the surface color represents the displacement in the y direction. Figures 3(a) and 3(d) show the wave structures for the S0 mode. From these figures, we can see energy leakage to the lower region, but attenuation cannot be seen clearly in the plate. This means that the S0 mode within the frequency ranges has small attenuation, as seen in the attenuation curves of Fig. 2(b). The A0 mode in Figs. 3(b) and 3(e) mainly vibrates in the thickness direction over the whole cross section of the plate, and energy leaks out to the water as a plane wave. The amplitude decreases as it propagates in the x direction in the plate, while the A0 mode attenuates due to the leakage. It can be seen in the wave structures in Figs. 3(c) and 3(f) that the quasi-Scholte wave propagates at the water–plate interface with large vibration in the x direction. The vibration spreads over the entire cross section of the plate in the low frequency range [Fig. 3(c)], while the vibration localizes at the water–plate interface in the higher frequency range [Fig. 3(f)]. Therefore, the wave structure of the quasi-Scholte wave is strongly dependent on frequency although attenuation is zero over the whole frequency range and dispersion is small beyond a certain frequency.

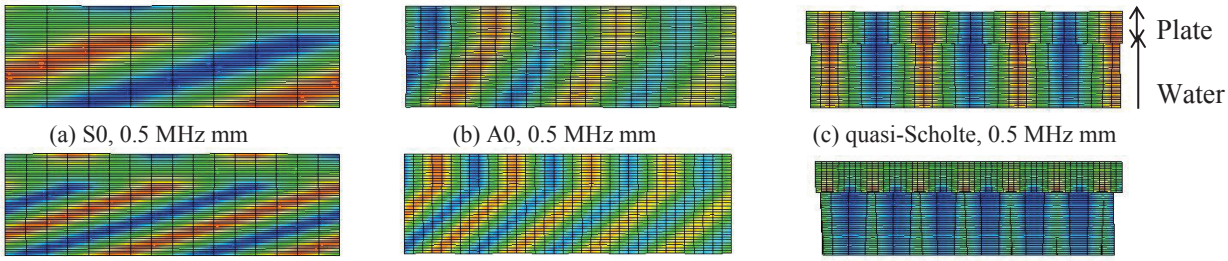

(a) S0, 0.5 MHz mm (b) A0, 0.5 MHz mm (c) quasi-Scholte, 0.5 MHz mm

(d) S0, 1 MHz mm (e) A0, 1 MHz mm (f) quasi-Scholte, 1 MHz mm

FIGURE 3. Wave structures at the selected points shown in Fig. 2.
The surface color denotes displacement in the thickness direction.

Next, waveforms in the time domain for external transient loading obtained by Eq. (4) are discussed. The upper traction-free surface of a 1 mm thick steel plate is subjected to external loading at $x = 0$ in the y direction. The input waveforms are Gaussian burst waves with central frequencies of 0.5 MHz and 1.0 MHz. Figure 6 shows the transient responses of the y-directional displacement on the lower water-coupled surface at x = 50, 100, 150, 200 mm. These waveforms are normalized by the maximum peak-to-peak amplitude of the y-directional displacement at the source point $x = 0$ (A_{in},), and the length of the y axes in both figures is set to $1/2A_{in}$. Then we can compare Figs. 6(a) and 6(b) showing the waveforms at the different frequencies. The oblique lines stand for the arrival times of the S0, A0, and quasi-Scholte waves predicted by the group velocities at the center frequencies. The figures show that the three modes are recorded in both frequency ranges and the A0 modes attenuate significantly, while the quasi-Scholte waves keep their waveforms as they propagate. These results are also predicted by dispersion curves and attenuation curves, as shown previously. From the viewpoint of long-range inspection for a steel plate, the quasi-Scholte wave is suitable due to the characteristics of zero attenuation and low dispersion.

Comparing the quasi-Scholte waves in Figs. 6(a) and 6(b), displacements at 0.5 MHz are larger than those in 1.0 MHz. This is because the generation efficiency of quasi-Scholte waves is strongly dependent on frequency. It is known that applying external loading similar to the wave structure of a certain mode of Lamb wave can generate the mode efficiently [12]. Because the mode shown in Fig. 3(c) distributes vibration over whole plate thickness, the quasi-Scholte wave in the low frequency range can be generated efficiently by loading on the upper surface. On the other hand, external loading on the upper surface cannot generate the quasi-Scholte wave efficiently in the high frequency range because it has a localized vibration on the lower surface in the high frequency range.

However, waves localized at the inner surface are generally more sensitive to inner defects. That is, when we consider the inspection of inner defects in a pipe and a tank, a quasi-Scholte wave in the higher frequency range improves the detectability of inner defects. Considering both generation efficiency and defect detectability, we need to determine an appropriate frequency range to use the quasi-Scholte wave for the inspection of inner defects. Since we drew the same conclusion for aluminum plates in Ref. [2], this result will apply in general to metallic plates having largely different acoustic impedances and sound speeds as compared with those of water.

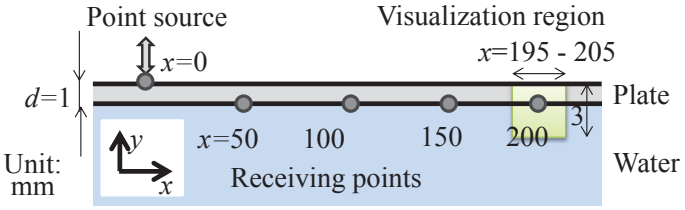

FIGURE 4. Calculation settings for transient analysis.

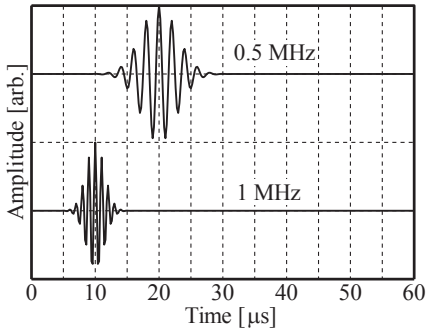

FIGURE 5. Incident waveforms at two different frequencies.

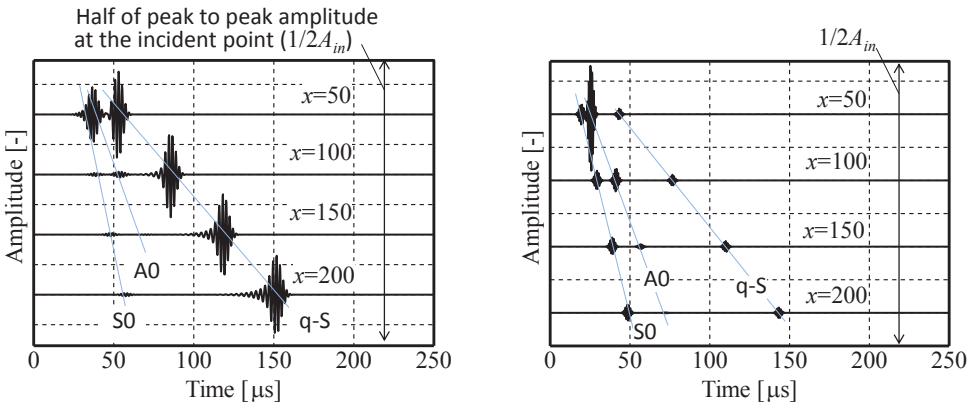

(a) 0.5 MHz (b) 1.0 MHz

FIGURE 6. Displacement in the thickness directions at the four points shown in Fig. 4 for a steel plate The length of the *y* axis is half of the peak-to-peak amplitude at the incident point.

LAMB WAVES IN A RESIN PLATE LOADED WITH FLUID ON A SINGLE SURFACE

Pipes made of resin such as polyvinyl chloride (PVC) and polyethylene (PE) are widely used for fluid transport pipe systems. Since resin generally has low longitudinal and transverse velocities close to the sound speed of water, we can expect that the wave propagation in a resin plate is vastly different from that in a metallic plate. Therefore, in this section we discuss results with SAFE calculations for a PVC plate (longitudinal wave velocity c_L = 2400 m/s, transverse wave velocity c_T = 1100 m/s, density ρ_s= 1400 kg/m^3) loaded with water on a single surface.

Figure 7 shows group velocity dispersion curves and attenuation curves of Lamb waves in a PVC plate. The modes having attenuation below 200 are shown in these figures, as in Fig. 2. Three modes labeled as mode 1, 2, and 3 exist at 0.5 MHz mm. Mode 1 resembles the S0 mode of the Lamb wave that has high group velocity close to the longitudinal wave velocity, and modes 2 and 3 (drawn in blue lines) have zero attenuation. Figure 8 shows wave structures of modes 1, 2, and 3 at 0.5 MHz mm and of modes 2 and 3 at 1.0 MHz mm. Surface color is a displacement in the *y* direction, as in Fig. 3. Mode 1 is similar to an S0 mode of the Lamb wave in that group velocity is close to the longitudinal wave velocity, but it differs from an S0 mode in that attenuation due to energy leakage to water is very large. Mode 2 in Figs. 8(b) and 8(d) vibrates locally at the upper and lower surfaces, which seems like a mixed mode of Rayleigh waves and quasi-Scholte waves. Mode 3 has a similar group velocity dispersion curve with that of an A0 mode of a Lamb wave but has zero attenuation. Wave structures of mode 3, shown in Figs. 3(c) and 3(f), resemble those of quasi-Scholte waves in the plates, but the vibration in water is small.

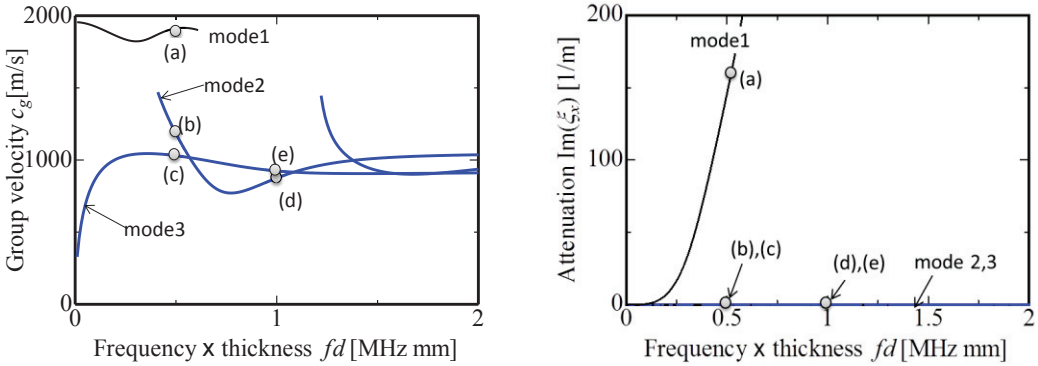

(a) Group velocity dispersion curves. (b) Attenuation curves.

FIGURE 7. Dispersion curves for a water-loaded PVC plate.

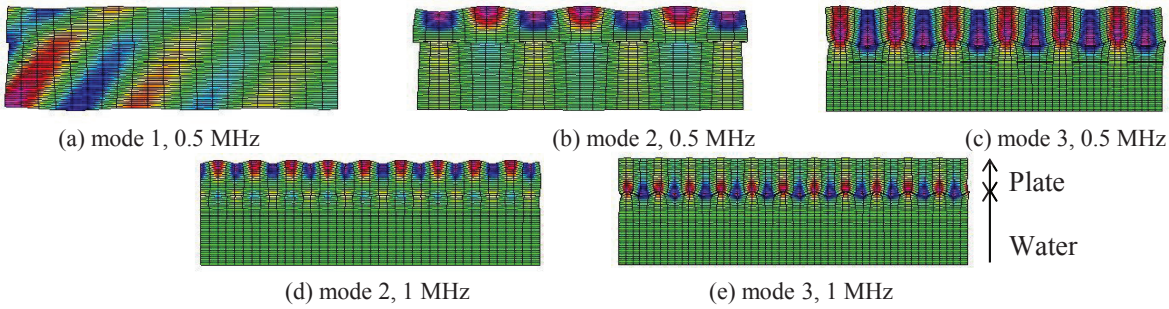

FIGURE 8. Wave structures at the selected points shown in Fig. 8.
Surface color denotes displacement in the thickness direction.

Next, transient responses for a 1 mm thick PVC plate coupled with water on a single side are shown in Fig. 9. These waveforms have a y-directional displacement at four points on the lower surface for the incidence of $x = 0$ at 0.5 MHz and 1.0 MHz central frequencies, as shown in Fig. 6 for a steel plate. The lengths of the y axes in both figures are also half of the displacement at the incident position $1/2A_{in}$. Two modes can be seen in both figures: one is the high dispersive mode 2 and the other one is the low dispersive mode 3. The other modes cannot be obtained due to their large attenuation. Comparing Fig. 9(a) with Fig. 9(b), the low dispersive mode 3 in Fig. 9(a) is larger than mode 3 in in Fig. 9(c). This is because the generation efficiency of mode 3 differs in frequency like the quasi-Scholte wave for a steel plate.

We can expect that these non-attenuated modes are suitable for the long-range inspection of a PVC plate. In particular, the low dispersive mode 3 is preferable. However, since mode 3 has less generation efficiency in the higher frequency range t, we need to find an appropriate frequency range to detect inner defects in a PVC plate, too.

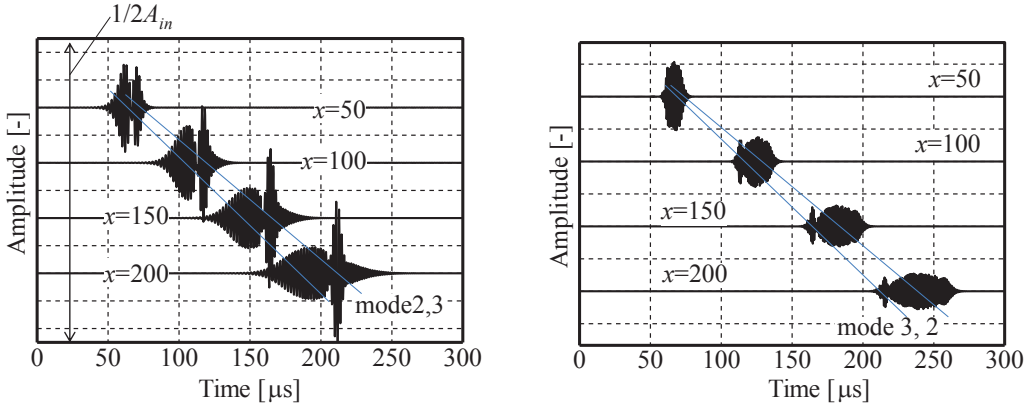

(a) 0.5 MHz (b) 1.0 MHz

FIGURE 9. Displacement in the thickness directions for the four points shown in Fig. 4 for the PVC plate.
The length of the y axis is half of the peak-to-peak amplitude at the incident point.

CONCLUSIONS

This study discussed Lamb waves in water-loaded plates using SAFE calculations. In particular, assuming the inspection of inner defects in pipes and tanks filled with water, we presented results of transient responses for dynamic loading subjected to steel and PVC plates loaded with water on a single surface.

The results showed that the quasi-Scholte wave is useful because the non-attenuated and low dispersive mode can propagate for long distances in such water-loaded steel plates. Since the generation efficiency and detectability of inner defects are dependent on frequency in the quasi-Scholte wave, we need to find an appropriate frequency range to use the quasi-Scholte wave. For a PVC plate, we obtained very different dispersion curves, attenuation curves, and wave structures from those of a steel plate. There existed a plural number of non-attenuated modes. We

expect that one of them is promising for long-range inspection due to its low dispersive nature. However, since the non-attenuated and low dispersive mode was dependent on frequency in its wave structures, such as a quasi-Scholte wave in a water-loaded steel plate, the appropriate frequency range should be based on the generation efficiency and defect detectability.

ACKNOWLEDGMENTS

This work was supported by JSPS KAKENHI Grant Number 26282094. The authors would like to thank Professor Shiro Biwa for his continuing encouragement.

REFERENCES

1. T. Hayashi and D. Inoue, Ultrasonics **54**, 1460–1469 (2014).
2. D. Inoue and T. Hayashi, Ultrasonics **62**, 80–88 (2015).
3. L. Gavrić, J. Sound Vib. **185**, 531–543 (1995).
4. L. Gray, J. Sound Vib. **195**, 477–505 (1996).
5. D. J. Thompson and C. J. C. Jones, J. Sound Vib. **253**, 401–419 (2002).
6. P. W. Loveday, IEEE Trans. Ultrason. Ferroelectr. Freq. Control **55**, 2038–2045 (2008).
7. M. Castaings and M. Lowe, J. Acoust. Soc. Am. **123**, 696–708 (2008).
8. Z. Fan, M. Lowe, and M. Castaings, J. Acoust. Soc. Am. **124**, 2002–2010 (2008).
9. F. Treyssède, K. L. Nguyen, A.-S. Bonnet-BenDhia, and C. Hazard, Wave Motion **57**, 1093–1107 (2014).
10. M. Mazzotti, A. Marzani, I. Bartoli, and E. Viola, Int. J. Solids Struct. **49**, 2359–2372 (2012).
11. M. Mazzotti, I. Bartoli, A. Marzani, and E. Viola, Ultrasonics **53**, 1227–1241 (2013).
12. T. Hayashi, C. Tamayama, and M. Murase, Ultrasonics **44**, 17–24 (2006).